Annu. Rev. Fluid Mech. 2003. 35:441–68
doi: 10.1146/annurev.fluid.35.101101.161122

SHELL MODELS OF ENERGY CASCADE IN TURBULENCE

Luca Biferale
Department of Physics and INFM, University of Rome, Tor Vergata, Via della Ricerca Scientifica 1, 00133 Rome, Italy; email:biferale@roma2.infn.it

Key Words dynamical models, multifractals

■ **Abstract** We review the most important theoretical and numerical results obtained in the realm of shell models for the energy-turbulent cascade. We mainly focus here on those results that had or will have some impact on the fluid-dynamics community. In particular, we address the problem of small-scale intermittency by discussing energy–helicity interactions, energy-dissipation multifractality, and universality of intermittency, i.e., independence of anomalous scaling exponents from large-scale forcing and boundary conditions. A multifractal-based description of multiscale and multitime correlation functions in turbulence is also presented. Finally, we also briefly review the analytical difficulties, and hopes, of calculating anomalous exponents.

1. INTRODUCTION

Three-dimensional turbulence is considered one of the most important problems in classical physics still lacking both solid theoretical and phenomenological understanding in many applied and ideal situations (Frisch 1995, Pope 2000, Bohr et al. 1998). In many cases, most problems can be traced to the lack of a clear theoretical understanding of the energy-cascade mechanism, i.e., of the mechanism that sustains turbulence on a wide range of scales.

In this paper we review the most important results obtained in modeling the energy-cascade mechanism by using a class of dynamical deterministic models also known as shell models. We focus mainly on those problems, and answers, that had, or may have, an impact on the traditional turbulent community. In a nutshell, the idea is to investigate the energy-cascade mechanism by a set of coupled nonlinear ordinary differential equations labeled by the index n (shell index):

$$\left(d/dt + \nu k_n^2\right)u_n = k_n G_n[u, u] + f_n, \tag{1}$$

where the dynamical (complex) variable, $u_n(t)$, represents the time evolution of a velocity fluctuation over a wavelength $k_n = k_0\lambda^n$, with λ, the intershell ratio, usually set to 2.

Velocity evolution is followed only over a set of shells logarithmically equispaced. Wavenumbers are scalars. Geometry is lost. The nonlinear coupling $G_n[u, u]$ is chosen so as to preserve total energy, helicity, and volume in phase space as for the original nonlinear terms of NS equations. Large-scale boundary conditions are imposed by demanding that fluctuations do not exist on scales larger than a fixed typical integral scale $L_0 = 1/k_0$, i.e., $u_n = 0$ for $n < 0$. The viscous mechanism on the left-hand side of Equation 1 is such to enforce a stretched exponential decaying of u_n for k_n large enough. The forcing term, f_n, is usually chosen with support only at large-scale (small-shell) indices if one aims to mimic a large-scale forced turbulence. Moreover, usually, though not necessarily, one enforces locality of interactions in Fourier (shell) space by demanding that the nonlinear function $G_n[u, u]$ couples only close-by scales (say, nearest and next-to-nearest shells).

Shell models go back to the pioneering works of Lorenz (1972), Siggia (1978), and the Russian school (Desnyansky & Novikov 1974, Gledzer 1973). The rationale behind shell models is clear. We need a simple model, dimensionally consistent with (but simpler than) NS equations, able to describe a dynamical deterministic evolution of a set of variables on a wide range of scales and with a wide range of characteristic times. In other words, one wants to define a model able to describe the analogue of the phenomenological Richardson cascade but possessing a deterministic time evolution.

Shell-models pluses are many. Among them, we cite the moderate number of degrees of freedom, $\#_{dof}$, needed to reach high Reynolds numbers. In shell models the $\#_{dof}$ grows only logarithmically in Reynolds different from the NS case, where we have: $\#_{dof} \propto Re^{9/4}$. The small $\#_{dof}$ needed to obtain high Reynolds numbers must not lead to the false conclusion that numerical simulations of shell models are easy to perform. Indeed, also in shell models we have the same singular dependency of the smallest eddy-turnover time on Reynolds numbers present in NS equations. Performing numerical simulations at high Reynolds numbers needs extremely small time discretization in shell models. The other important plus, which is less recognized, is the absence of sweeping effects, i.e., the absence of a direct coupling between integral scales and inertial scales. Shell models are the ideal place where nontrivial time properties of the energy-cascade mechanism can be studied, measured, and, hopefully, analytically calculated, because time fluctuations are not hidden by the large-scale sweeping, which is different from what happens in any Eulerian measurement of three-dimensional turbulence. Shell models provide the models closest to the time evolution of a velocity field in a Lagrangian, or quasi-Lagrangian, reference frame (Belinicher et al. 1987) also retaining fluctuations on a wide range of scales.

Of course, there are also some minuses. Among them, we cite the obvious absence of any geometrical effect (although shell models meant to describe either a one-dimensional cut of a three-dimensional field or the whole three-dimensional field have also been studied. See Benzi et al. 1996, Grassmann & Lohse 1994) and, somehow connected to it, the absence of pressure. Still, pluses overwhelm

minuses, at least if one does not ask of shell models answers they cannot provide.

The paper is organized as follows: In Section 2 we briefly introduce the class of shell models that is the chief subject of this review. In Section 3 we review the most interesting numerical results obtained concerning the presence of small-scale intermittency in the energy cascade, including the possible connection with small-scale helicity (Subsection 3.2) and the important issue of universality, i.e., dependency/independence on/off large-scale forcing and boundary conditions (Subsection 3.4). In Section 4 we review what is known, or measured, about multitime, multiscale correlation functions in shell models with some emphasis on their connection with the equivalent observable in NS equations and with their estimate in terms of multifractal measures and multiaffine processes. In Subsection 4.4 we switch to questions for the future. In particular we discuss how the problem of calculating, from first principle, anomalous scaling exponents is tightly connected to a precise control of multitime, multiscale statistics not only asymptotically, i.e., not only for large-scale separation and for large time lags. We conclude in Section 5 with a few suggestions for experimentalists and a "guided tour to further reading" on shell models works that are worth citing to emphasize other possible fields of application.

2. SHELL MODELS

The phenomenological and kinematical constraints to have a short-range, quadratic nonlinearity preserving total energy, total helicity, and phase-space evolution do not fix in a unique way the form of the $G_n[u, u]$ term in the equation of motion (Equation 1). We concentrate here mainly on one model, the GOY model (Gledzer 1973, Ohkitani & Yamada 1989) because its rich temporal and multiscale statistics possess many striking similarities with real turbulent flows. GOY model is defined as:

$$\left(d/dt + \nu k_n^2\right)u_n = i\left(k_n u_{n+2}^* u_{n+1}^* - b k_{n-1} u_{n+1}^* u_{n-1}^* + c k_{n-2} u_{n-1}^* u_{n-2}^*\right) + f_n, \quad (2)$$

where the velocity-shell variable u_n is a complex variable and the free parameters b, c are connected to the physical dimensions of the inertial quadratic invariants. It is easy to realize that in the inviscid and unforced limit $\nu = f_n = 0$, Equation 2 has two global quadratic invariants of the form $Q_{1,2} = \sum_n k_n^{x_{1,2}} |u_n|^2$. By requiring that one coincides with the total energy

$$Q_1 \equiv E = \sum_n |u_n|^2,$$

one needs to fix $c = -(1 - b)$. With this choice, the second invariant is not positive-defined (when $0 < b < 1$) and has the form

$$Q_2 = \sum_n (-)^n k_n^{x(b,\lambda)} |u_n|^2$$

with

$$x(b, \lambda) = -\log_\lambda |1 - b|. \tag{3}$$

(For $b > 1$ the second invariant also becomes positive-defined; shell models in such a range of parameters have been studied in order to reproduce some feature of two-dimensional turbulence (see Aurell et al. 1994a, Ditlevsen & Mogensen 1996). A particularly appealing choice consists in choosing the second invariant to have the same physical dimensions as NS helicity, $x(b, \lambda) = 1$, which gives for the popular choice of intershell ratio $\lambda = 2$, the value $b = 1/2$. The possibility of changing the physical dimensions of the second invariant, keeping total energy preserved, has stimulated many theoretical and numerical investigations targeted at understanding the interplay between the energy-cascade mechanism and helicity or generalized helicity transfer (Biferale & Kerr 1995, Frick et al. 1995, Benzi et al. 1996a, Ditlevsen 1997).

Another striking and important similarity to NS equations is the existence of two exact inertial laws (Pisarenko et al. 1993; Biferale et al. 1998a,b) that are the equivalents of the $4/5$ (see Frisch 1995) and the $2/15$ law (Chkhetiani 1996), which fix the scaling of third-order correlation entering in the NS energy and helicity fluxes, respectively. Indeed, it is easy to derive two exact equations for energy and helicity fluxes throughout shell number N:

$$\frac{d}{dt}\sum_{n=1}^{N} E_n = k_N \langle \Pi_N^E \rangle - \nu k_N^2 \sum_{n=1}^{N} E_n + E_{in}, \tag{4}$$

$$\frac{d}{dt}\sum_{n=1}^{N} H_n = (-)^N k_N^2 \langle \Pi_N^H \rangle - \nu k_N^2 \sum_{n=1}^{N} H_n + H_{in}, \tag{5}$$

where E_n, H_n are the energy and helicity of the nth shell, respectively: $E_n = \langle |u_n|^2 \rangle$, $H_n = (-)^n k_n \langle |u_n|^2 \rangle$ and E_{in}, H_{in} are the input of energy and helicity due to forcing effects. In Equations 4 and 5 we have introduced the triple-correlation function defining the energy flux:

$$\langle \Pi_N^E \rangle = \left\langle \Im \left(u_{n+2} u_{n+1} u_n + \frac{(1-b)}{\lambda} u_{n+1} u_n u_{n-1} \right) \right\rangle, \tag{6}$$

and the helicity flux:

$$\langle \Pi_N^H \rangle = \left\langle \Im \left(u_{n+2} u_{n+1} u_n - \frac{b\lambda + 1}{\lambda^2} u_{n+1} u_n u_{n-1} \right) \right\rangle. \tag{7}$$

Let us now fix the scale k_N in the inertial range in Equation 5. By sending the viscosity to zero, noticing that energy/helicity inputs E_{in}, H_{in} are scale independent (if forcing, f_n, is concentrated only at large scales) and supposing the existence of a stationary state, we derive from Equations 4 and 5 two exact scaling laws for the two different triple correlations entering in energy and helicity flux, respectively:

$$\langle \Pi_N^E \rangle \sim k_N^{-1} E_{in}, \quad \langle \Pi_N^H \rangle \sim k_N^{-2} H_{in}. \tag{8}$$

Another important general property shared by almost all shell models is the presence of a phase-invariance that constrains the possible set of stationary correlation functions with a nonzero mean value. In particular, it is simple to realize that the GOY equations of motion are invariant (neglecting the forcing mechanism) under the following redefinition of the phase variables (Benzi et al. 1993):

$$u_n \to u_n \exp^{i\theta_n}, \tag{9}$$

with the only constraint that $\theta_{n+2} + \theta_{n+1} + \theta_n = 0, mod(2\pi)$. Owing to this phase invariance, the only quadratic form in the shell-velocity field with a mean value different from zero is $\langle u_n u_{n+3m} \rangle$ or $\langle u_n u_n^* \rangle$. Similarly, there are other constraints for three-point correlation fuctions and many-point correlation functions. This phase invariance is the equivalent of Galilean invariance in NS equations. Phase invariance can be exploited to define a slightly different version of the GOY model (L'vov et al. 1998a) that further reduces the number of possible nonzero correlation functions. This new model differs from the GOY model only for the structure of complex conjugation in the nonlinear term, namely,

$$\left(d/dt + \nu k_n^2\right) u_n = i\left(k_n u_{n+2} u_{n+1}^* - b k_{n-1} u_{n+1} u_{n-1}^* - c k_{n-2} u_{n-1} u_{n-2}\right) + f_n. \tag{10}$$

The Equation 10 model has the same phase invariance as Equation 9 except that the constraint between three consecutive phases becomes $\theta_{n+2} - \theta_{n+1} - \theta_n = 0$ $mod(2\pi)$. Such a small change simplifies significantly the spectrum of possible correlation functions. The only nonzero quadratic forms are fully local in wave number, $\langle u_n u_n^* \rangle$; the same is true for three-points correclation functions, $\langle u_{n+2}^* u_{n+1} u_n \rangle$. Also, four-points correlation functions are local except for the possibility of having two-velocity amplitude at two different scales, $\langle |u_n|^2 |u_m|^2 \rangle$ (L'vov et al. 1998a). Phenomenology of the GOY model and of its new version (Equation 10) are the same, and most of the quantitative results coincide exactly. The advantage of the new version is that numerical results are cleaner, thanks to the strong statistical locality induced by the phase invariance. This new version also looks more attackable from a field-theoretical point of view, although we still lack a systematic, controlled procedure to implement field-theoretical methods (see Section 5 for more details). Hereafter, we mainly discuss theoretical, phenomenological, and numerical results within the realm of the Equation 10 model.

3. SMALL-SCALES INTERMITTENCY AND UNIVERSALITY OF ANOMALOUS EXPONENTS

We now start by discussing what is, by far, the most striking statistical properties of the Equations 2 and 10 models and the connections with the analogue properties of NS equations.

The simplest set of correlation functions able to quantify the statistical properties of the energy cascade in the original NS equations are the so-called longitudinal-structure functions, $S_p(R)$, i.e., moments of velocity differences over a scale R in

the direction of $\hat{R}$:

$$S_p(R) = \langle [(\mathbf{v}(\mathbf{x}+\mathbf{R}) - \mathbf{v}(\mathbf{x})) \cdot \hat{\mathbf{R}}]^{\mathbf{p}} \rangle,$$

where we have neglected any dependency on $\mathbf{x}$ and on the direction of $\mathbf{R}$ because we are supposedly dealing with an isotropic and homogeneous ensemble. The equivalent of the NS structure functions in shell models is given simply by

$$S_p(k_n) = \left\langle |u_n|^p \right\rangle, \tag{11}$$

or, similarly, in terms of energy-flux moments (Equation 7), by

$$S^q_\Pi(k_n) = \left\langle \Pi_n^{q/3} \right\rangle. \tag{12}$$

Dimensional arguments, à la Kolmogorov, predict a simple, nonanomalous scaling in the inertial range of NS turbulence:

$$S_p(R) = \langle (v(x+R) - v(x))^p \rangle \sim \epsilon^{\frac{p}{3}} R^{\frac{p}{3}}, \tag{13}$$

where ϵ is the rate of energy dissipation. Similarly, dimensional analysis can be rephrased to shell models, obtaining:

$$S_p(k_n) \sim S^p_\Pi(k_n) \sim k_n^{-\frac{p}{3}}. \tag{14}$$

As is well known (Frisch 1995), Kolmogorov prediction in Equation 13 is not supported either by experiments or by numerics in NS turbulence, except for the exact value given by the 4/5 law, $S_3(R) = -\frac{4}{5}\epsilon R$. In particular, Kolmogorov prediction fails to describe intermittency of the energy cascade. With energy-cascade intermittency, we mean the existence of a whole spectrum of anomalous scaling exponents, $\zeta^{NS}(p)$, different from the K41, $p/3$ law:

$$S_p(R) = \langle [(\mathbf{v}(\mathbf{x}+\mathbf{R}) - \mathbf{v}(\mathbf{x})) \cdot \hat{\mathbf{R}}]^p \rangle \sim R^{\zeta^{NS}(p)}. \tag{15}$$

Some updated values for the lowest order of scaling exponents are: $\zeta^{NS}(2) = 0.7(2)$, $\zeta^{NS}(3) = 1$ (exact), $\zeta^{NS}(4) = 1.27(3)$, $\zeta^{NS}(5) = 1.53(4)$, and $\zeta^{NS}(6) = 1.78(6)$ (van de Water & Herweijer 1996). Strikingly enough, the pioneering work of Jensen, Paladin, and Vulpiani (Jensen et al. 1991) also showed that the GOY model possesses a very similar quantitative and qualitative intermittency. By defining anomalous exponents for the shell model as

$$S_p(k_n) = \left\langle |u_n|^p \right\rangle \sim k_n^{-\zeta^{SM}(p)}, \tag{16}$$

one measures numbers that are almost indistinguishable from the NS case, i.e., $\zeta^{NS}(p) = \zeta^{SM}(p)$, within error bars, at least by fixing the free parameters in the model to be on the helicity-preserving curve (Equation 3) (Jensen et al. 1991, Pisarenko et al. 1993, Kadanoff et al. 1995). This result was impressive, and it renewed great interest in shell models on the part of both communities working on dynamical systems and turbulence.

Energy-cascade intermittency, i.e., the existence of anomalous scaling exponents, must never be underestimated. It has a series of consequences for almost

any community working in the field. Let us go through some of them by showing the similarities between the NS case and the shell model results.

3.1. Small-Scale PDFs

Anomalous exponents mean that velocity-different probability density functions (PDFs) cannot be simply rescaled with a unique scale-dependent function, i.e., PDFs of velocity increments rescaled to have a fixed variance do not collapse by changing the scale. In particular, intermittency implies that velocity fluctuations become more and more non-Gaussian by decreasing the scale, as it is easily quantified by looking at the behavior of velocity kurtosis, $K(R)$, and/or skewness, $S(R)$, at scale R:

$$K(R) \equiv \frac{S_4(R)}{S_2(R)^2} \sim R^{-0.13} \quad S(R) \equiv \frac{S_3(R)}{S_2(R)^{3/2}} \sim R^{-0.05}, \tag{17}$$

where the scaling exponents have been deduced from the $\zeta^{NS}(p)$ values given above. A direct consequence of intermittency is that even at very small scales, say, the Kolmogorov scale, one may observe velocity fluctuations that are of the order of the large-scale velocity root mean squared (Noullez et al. 1997), something that cannot be neglected by anybody who needs to model small-scale effects in any applied or theoretical problem. Exactly the same phenomenon happens in shell models. By measuring shell-variable PDFs in the inertial range, a clear trend toward a less and less Gaussian behavior is depicted (see Figure 1).

In order to appreciate the statistical confidence typical of shell-model inertial range quantities, we also plot in Figure 2 the scaling laws of two structure functions, $S_4(k_n)$ and $S_6(k_n)$. Clearly, scaling properties are extremely good.

The main advantage of studying small-scale fluctuations in shell models is the possibility of pushing the numerics to Reynolds numbers values that are unthinkable for the original NS case. Therefore, any small-scale modelization can be checked with a much higher degree of confidence than in direct numerical simulation (DNS) of a three-dimensional flow. For example, one theoretical and applied issue connected to small-scale intermittency is whether inertial range statistics are independent or not of the small-scale energy-draining mechanism, i.e., whether it is used viscosity, hyperviscosity, or eddy-viscosity. See (Pope 2000) for a recent introduction. While the numerical evidence in NS equations is not conclusive (Borue & Orszag 1995, Cao et al. 1996), we are quite confident that inertial-range intermittency in shell models is ultraviolet robust, i.e., does not depend on the detailed mechanism used to dissipate energy at small scales (Benzi et al. 1999, L'vov et al. 1998b).

3.2. Energy-Helicity Interaction

It is well known that NS configurations carrying a strong positive or negative helicity have a depleted energy transfer (Moffat 1969, Waleffe 1993). The reason is that owing to different scaling properties (see Equation 7) it is impossible

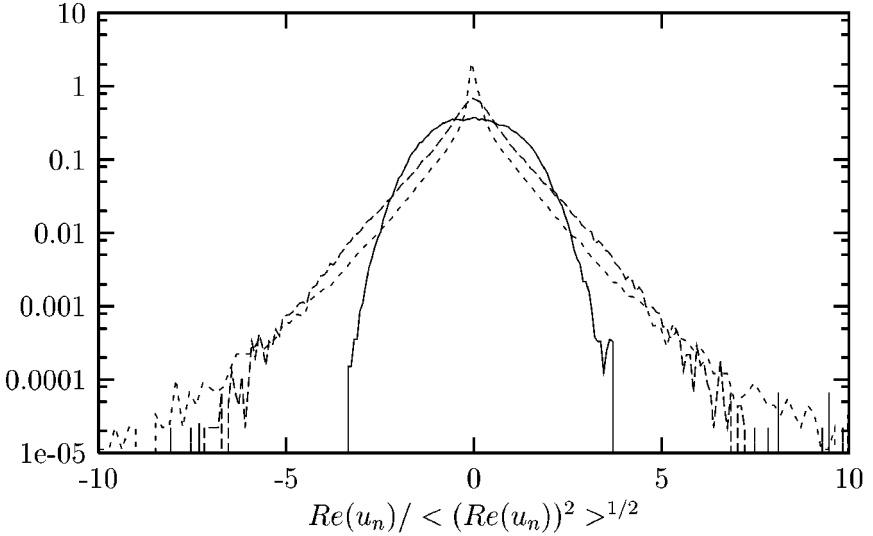

Figure 1 Normalized PDFs of the real part of shell-model variables, $Re(u_n)$ at wave number k_n with $n = 5, 10, 15$. The largest scale $n = 5$ is given by the *solid line*; the intermediate scale $n = 10$ is the *long-dashed line*; the smallest scale, $n = 15$ is the *short-dashed line*. Notice the same trend toward a more and more non-Gaussian distribution, by decreasing the scale, measured in experimental PDFs (Noullez et al. 1997).

to transfer downscale simultaneously both energy and a coherent (with a definite sign) helicity fluctuation. Studies of helical NS turbulence are particularly difficult numerically because of the highly fluctuating helicity signal, and experimentally because of the difficulty in measuring simultaneously the three vorticity- and velocity-field components (Moffat & Tsinober 1992). Shell models offer, unlike NS equations, an ideal case where the statistical correlation between energy and helicity may be studied with high numerical accuracy on a wide range of scales.

To this purpose, it is better to slightly modify the structure of a GOY shell model in such a way as to include explicitly two shell variables, u_n^+ and u_n^-, carrying positive and negative helicity, respectively (Benzi et al. 1996a). In this way, one constructs a shell model with exactly the same helical structure as the Fourier-helical decomposed NS equations (Waleffe 1992, 1993).

Indeed, in Kadanoff et al. (1995) first, and in Biferale & Kerr (1995) and Benzi et al. (1996) later, it was shown that large-scale helicity plays a crucial role in determining the statistical properties of the energy cascade. Some numerical exploration has also suggested that helicity flux, in the presence of large-scale helicity pumping, is Reynolds independent (Biferale et al. 1998b) and that it is a good approximation to consider small-scale helicity being passively advected by the energy-carrying velocity field (Borue & Orszag 1997, Biferale et al. 1998a).

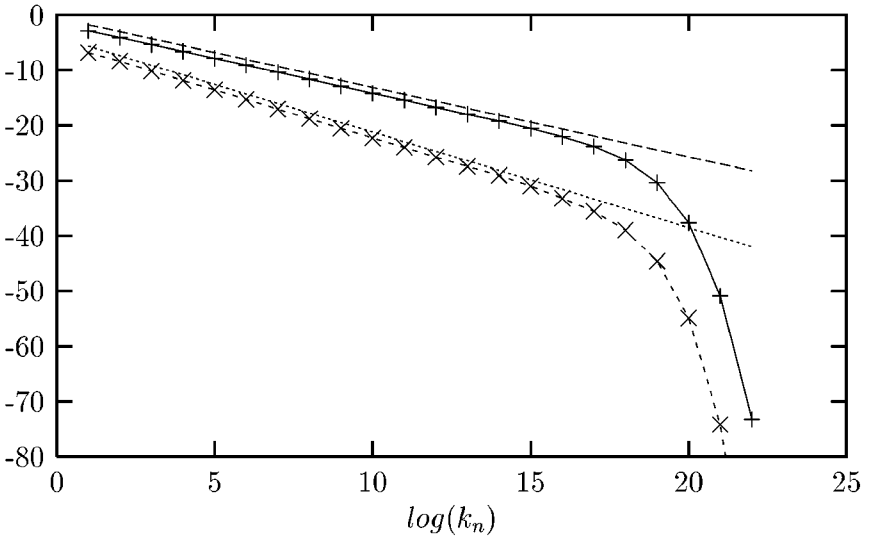

Figure 2 Example of a typical scaling laws for fourth order (+) and sixth order (×) structure functions. Straight lines are the best fit in the inertial range giving, respectively, the slopes $\zeta(4) = 1.26(3)$ and $\zeta(6) = 1.76(5)$. Numerical simulations has been done with a total number of shells $N = 25$, $\nu = 5.e-7$, $f_n = 0.1(1+i)\delta_{n,0}$, and $k_0 = 0.05$. Statistics has been collected for about 500 eddy-turnover times. Reynolds number measured on the gradients is $Re_\lambda \sim 5000$.

3.3. Energy Dissipation

Another interesting phenomenological issue with many counterparts in the NS field is connected to the energy-dissipation statistics. As first pointed out by Landau (Landau & Lifshitz 1987) in his celebrated critique of the K41 theory, energy-cascade intermittency must be somehow connected to some nontrivial spatial distribution of energy dissipation. This led first Kolmogorov (1962) and then others (Mandelbrot 1977, Parisi & Frisch 1985) to propose stochastic models for the energy cascade leading to log-normal, fractal, or even multifractal energy-dissipation statistics.

Intermittent energy dissipation observed in true NS equations has been successfully explained by the refined Kolmogorov hypothesis (RKH) (Kolmogorov 1962). The refined Kolmogorov hypothesis says that the coarse-grained energy dissipation ϵ_r, over a box $\Lambda(r)$ of size r, must be statistically connected to the velocity-increment fluctuation on the same distance, namely, by calling $\delta_r v = v(x+r) - v(x)$ the velocity increment on a distance r:

$$(\delta_r v)^3 \sim \epsilon_r r, \tag{18}$$

where $\epsilon_r = \frac{1}{r^3}\int_{\Lambda(r)} d^3x \epsilon(x)$. This relation is well satisfied experimentally and numerically (Stolovitzky & Sreenivasan 1994), leading to the natural linking

between inertial-range intermittency and multifractality of the coarse-grained energy dissipation. Indeed, from Equation 18 one readily obtains

$$\langle (\delta_r v)^p \rangle \sim \langle \epsilon_r^{p/3} \rangle r^{p/3} \sim r^{p/3+\tau(p)}, \tag{19}$$

where we have introduced the generalized fractal dimensions $\tau(p)$ that characterize the multifractality degree of the energy-dissipation measure (Meneveau & Sreenivasan 1987). RKH is a highly complex statistical and dynamical constraint that links dissipative and inertial physics in NS equations. By looking at the joint coarse-grained energy dissipation PDF in two different points, $P[\epsilon_r(x), \epsilon_{r'}(x')]$, one may investigate further spatial and/or scale dependencies of the energy-cascade mechanism (O'Neil & Meneveau 1993).

A shell model along a single chain as in the GOY model can show only energy-dissipation temporal intermittency. Indeed, Jensen et al. (1991) showed that energy-dissipation temporal fluctuations possess a highly nontrivial structure (see Figure 3 for a typical temporal evolution of $\epsilon(t) = \sum_n K_n^2 |u_n|^2$).

In order to study both RKH and energy-energy correlation problems, one needs to give a spatial structure to the shell model by jumping from a chain model to a tree model. This is achieved by letting grow the number of degrees of freedom with the shell index n as 2^n. The tree model can be regarded as describing the evolution of the coefficients of an orthonormal-wavelet $[\psi_{n,j}(x)]$ expansion of a one-dimensional projection of the velocity field (Nakano 1988, Muzy et al. 1993):

$$v(x,t) = \sum_{n=0}^{N} \sum_{j=0}^{2^n-1} u_{n,j}(t) \psi_{n,j}(x).$$

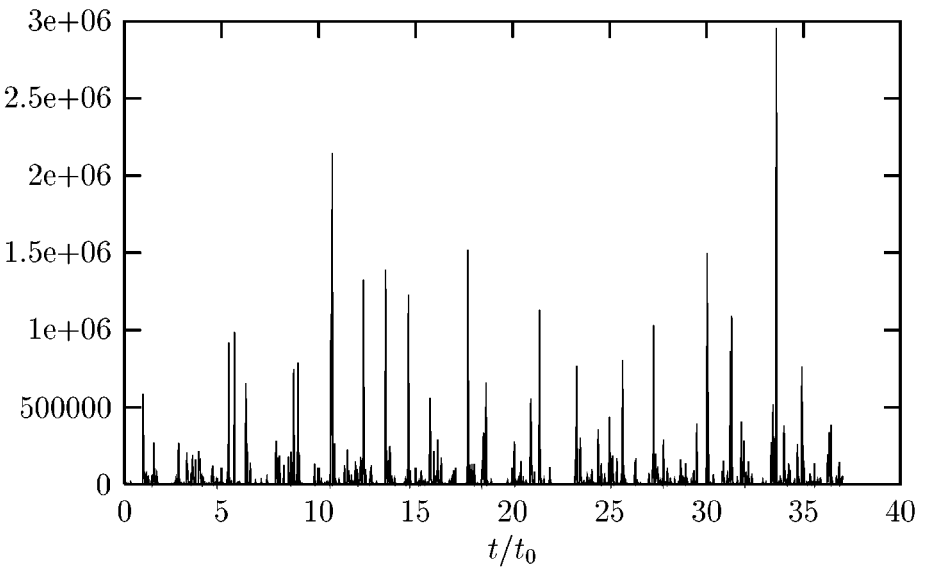

Figure 3 Typical time evolution of energy dissipation, $\epsilon(t) = \sum_n k_n^2 |u_n|^2$. Notice the extremely high intermittency.

We may write the tree model equation as:

$$d/dt\ u_{n,j} - \nu k_n^2 u_{n,j} = ik_n \sum_{n_1,n_2,j_1,j_2} \left[a_{n_1,n_2}^{j_1,j_2} u_{n_1,j_1}^* u_{n_2,j_2}^*\right] + \delta_{n_0,n} F, \qquad (20)$$

where the new index $j = 0, 2^n - 1$ labels the spatial position of eddies on each shell, F is some external forcing supposed to act only at large scales, and the coefficients $a_{n_1,n_2}^{j_1,j_2}$ are fixed by imposing conservation of helicity and energy in the inviscid unforced limit (Benzi et al. 1996b). The Equation 20 model has been shown to share both RKH Navier-Stokes and the complex energy-energy correlation structures, $\langle \epsilon_r^p(x) \epsilon_{r'}^q(x') \rangle$ with NS equations. In particular, experimental data suggest a dyadic ultrametric structure in the three-dimensional energy-cascade process (O'Neil & Meneveau 1993). Such a dyadic structure is highlighted by measuring correlation functions that strongly reflect the presence of quasi-discontinuities (fronts) in small-scale velocity configurations, as:

$$\left\langle \epsilon_r^p(x) \epsilon_r^{-p}(x') \right\rangle \sim r^{\phi(p)}. \qquad (21)$$

In O'Neil & Meneveau (1993), it has been shown that the scaling function, $\phi(p)$, in Equation 21 has a discontinuity in the derivative for $p = 1$. Similar results have been obtained in treelike shell models (see Figure 4), supporting the idea that the energy-cascade mechanism proceeds in a hierarchical way (ultrametric) in its route from large to small scales.

Other dynamical models on hierarchical structures have also been studied as an exact pruning from the NS possible interactions in Eggers & Grossman (1991), Aurell et al. (1994a,b), and Grossman & Lohse (1994).

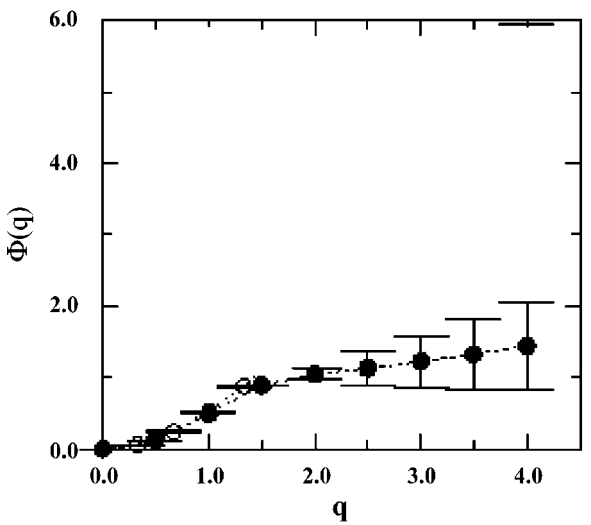

Figure 4 Scaling exponents, $\phi(q)$ defining the correlation $\langle \epsilon_r^q(x) \epsilon_r^{-q}(x') \rangle$ for $q = 1, \ldots, 4$. Experimental three-dimensional turbulent signal enjoys exactly the same behavior as shown in O'Neil & Meneveau (1993).

3.4. Universality of Small-Scale Fluctuations

We enter here into a very fundamental question that is connected to the robustness of small-scale statistical properties at changing the large-scale physics. General wisdom supports a strong universality hypothesis, i.e., the independence of anomalous scaling exponents from the large-scale forcing mechanism and the large-scale boundary conditions. Robustness of anomalous scaling exponents does not require that velocity-increment PDFs are universal at changing the large-scale boundary conditions. It only requires that given the large-scale fluctuations, i.e., given the large-scale velocity PDF, the relative way PDFs change at changing the scale is universal. Everything is quantitatively summarized by requiring that in writing $S_p(R) \sim C_p(R/L_0)^{\zeta(p)}$, we have universal scaling exponents $\zeta(p)$, and nonuniversal constants C_p. Universality of small-scale turbulence is a well-established result, corroborated by both experimental and numerical data, at least as far as isotropic fluctuations are involved (Benzi et al. 1995, van de Water & Herweijer 1996).

The importance of scaling-exponents universality should not be underestimated. It is the signature of two very important facts about NS equations. First, from a phenomenological point of view, it teaches us that dynamically (and statistically) speaking, the NS energy cascade is dominated by local or almost local interactions in the inertial range. Many successful stochastic multiplicative models to describe energy cascade are, indeed, based on this assumption. (Benzi et al. 1984, 1998; Renner et al. 2001). Second, from a more rigorous point of view, it teaches us that stationary correlation functions in the inertial range are dominated by zero-modes of the inertial operator, whereas dimensional scaling appears only as subleading contributions (if any).

Let us go through the two points above in some detail by looking at the results obtained in shell models. Here, again, shell models have played, and will play, a major role in fixing the problems, thanks to the high freedom we have in choosing large-scale forcing and boundary conditions and to the much higher accuracy with which we may measure small-scale fluctuations.

In Figure 5 we show the scaling properties of the sixth-order structure function in the modified GOY model Equation 10 at changing the large-scale forcing. As one can see, inertial-range behavior is strongly robust. Independently, on the forcing mechanism we soon recover, at scales small enough, the same scaling properties. Let us stress that this must be expected. The very existence of anomalous scaling laws cannot be connected to the forcing mechanism. This fact leads directly to the second matter we want to discuss. The main point is that the infinite hierarchy that must be satisfied by all velocity-correlation functions is linear, i.e., the time evolution of pth-order correlation functions depends linearly on the $(p+1)$th correlation function and on the velocity-forcing correlation.

We write, symbolically, the general equation that must be satisfied by the pth-order shell-correlation function, $C_p(k_{n_1}, k_{n_2}, \ldots, k_{n_p}) = \langle u_{n_1} u_{n_2} \ldots u_{n_p} \rangle$:

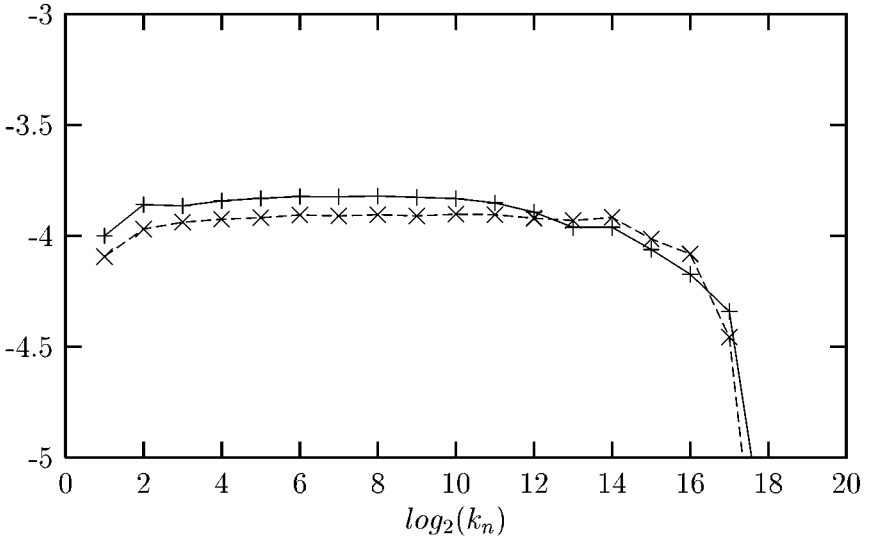

Figure 5 Compensated plot of sixth-order structure functions with the best-fit inertial range local slopes, $S^6(k_n)/k_n^{-\zeta(6)}$, for two different large-scale forcing. We used a forcing with no large-scale helicity, $H_{in} = 0$ (+) and a forcing with maximal large-scale helicity $H_{in} \sim E_{in}$ (×). In both cases we obtain the same scaling exponent in the inertial range, $\zeta(6) = 1.77(3)$. The parameters of the numerical simulations are the same as those of Figure 2.

$$0 = \frac{d}{dt} C_p(n_1, n_2, \ldots, n_p) = M^{p+1} C_{p+1}(n_1', n_2', \ldots, n_p') + F^{p-1,1}, \quad (22)$$

where we have indicated with M^{p+1} the linear operator coming from the nonlinear terms of Equation 10, and with $F^{p-1,1}$ the correlation between the $(p-1)$ velocity shell variables and the forcing term obtained directly from Equation 10. In Equation 22 we have neglected viscous contributions by assuming that all shells $n_1, \ldots, n_p$ are in the inertial range. We notice now that in the stationary regime we may interpret the constraints coming from the equations of motion as a nonhomogeneous linear system for the infinite set of correlation functions C_p for any p. The system is not closed, i.e., we have more unknowns than equations, and therefore very little can be said from the mathematical point (a difference from what happens in linear hydrodynamical problems describing passive quantities advected by turbulent velocity fields; see Section 4.4). In any case, one may still imagine that the solution will be composed of two contributions. One, C_{p+1}^{n-hom}, is given by a simple dimensional matching between the inertial operator and the nonhomogeneous forcing term:

$$M^{p+1} C_{p+1}^{n-hom} \sim F^{p-1,1}. \quad (23)$$

The second, C_{p+1}^{hom}, is given by a possible zero-mode of the inertial operator, i.e., by the homogeneous solution of the linear problem:

$$M^{p+1}C_{p+1}^{hom} = 0. \tag{24}$$

Nonhomogeneous contributions, if any, coming from a forced solution must possess a dimensional scaling. On the other hand, the homogeneous part must not satisfy any dimensional constraints. It may show, in principle, any anomalous scaling law. In particular, the fact that numerics show such a clear anomalous scaling is a clear indication that the physics, in the inertial range, is dominated by zero-modes and that dimensional scaling, if any, is always subleading:

$$C^{p+1}(k_n) \sim C_p^{hom}(k_n) + C_p^{non-hom}(k_n) \sim k_n^{-\zeta(p)} + k_n^{-\zeta_{dim}(p)}. \tag{25}$$

Such a mechanism, only phenomenologically consistent with what has been observed in NS equations and in shell models, can be pushed to a much higher degree of rigor in passive scalars/vectors advected by turbulent velocity fields. To show the consistency of the above description, one may perform two different decaying experiments (Biferale et al. 2002). In the first experiment, one follows the decaying in time of a set of velocity configurations coming from a forced stationary run. Namely, we integrate the decaying equations

$$\left(d/dt + \nu k_n^2\right)u_n = i\left(k_n u_{n+2}u_{n+1}^* - bk_{n-1}u_{n+1}u_{n-1}^* - ck_{n-2}u_{n-1}u_{n-2}\right) \tag{26}$$

by taking as the initial condition $u_n(t=0) = u_n^F$ with u_n^F chosen in the ensemble of forced stationary configurations. After averaging on the initial conditions, we can monitor the time evolution of any correlation function:

$$\frac{d}{dt}C_p(t) = M^{p+1}C_{p+1}(t) \tag{27}$$

with the initial condition $C_p(t=0) = C_p^{sta}$, where with C_p^{sta} we mean the stationary-correlation function (Equation 25) dominated by the anomalous zero-mode in the inertial range. In the second experiment, we follow exactly the same recipes except that we change, randomly, the phases of the initial conditions. In this way we change the initial ensemble of fields from the "correct" zero-mode of the inertial operator to something that has the same overall dimensions but with a completely wrong phase organization. In this second experiment we follow the evolution of Equation 27 but with a different initial condition: $C_p(t=0) = C_p^{ran}$. We expect two very different behaviors as a function of time in the two experiments. In the first, that is, the initial condition in the inertial range such that $M^{p+1}C^{p+1}(t=0) = 0$, we see some global time dependency only for times of the order of the largest eddy-turnover times, $\tau_0 \sim 1/(k_0 u_0)$, because only at large scales do we have a nonnegligible contribution from the dimensional, forced part $C_p^{non-hom}(k_n)$. On the other hand, in the second experiment, we have at the initial time, at all scales, $M^{p+1}C^{p+1}(t=0) \sim k_n^{(2-p)/3} \neq 0$, and therefore we expect a typical change of the correlation function in the inertial range over a much faster

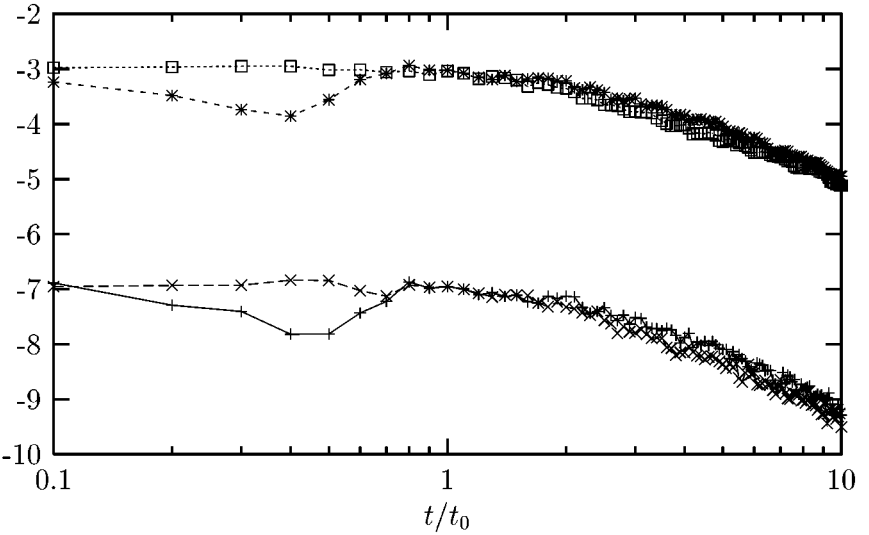

Figure 6 Comparison between the two decaying experiments. Time-evolution of $\langle |u_n|^4 \rangle(t)$ for shell $n = 5$ by averaging over the initial ensemble given by the stationary distributions (*top curve, squares*), or by averaging over a wrong initial ensemble with random phases (*top curve, stars*). *Bottom curves* are for shell variable $n = 15$: (stationary initial conditions, $\times$; random initial conditions, $+$). Notice that when we average, starting from the stationary set of configurations, the decaying sets up only for time larger than the large-scale eddy-turnover time t_0. Starting from a wrong ensemble, the correlation moves much sooner.

time, i.e., the local eddy-turnover time, $\tau_n \sim k_n^{-2/3}$. This is exactly what we found numerically, as can be seen in Figure 6. Such a result, with its counterparts for the NS equations (Biferale et al. 2002), gives strong support to the universality hypothesis.

4. MULTITIME MULTISCALE CORRELATION FUNCTIONS

In this section we focus on the problem of having a consistent phenomenological description of the energy-transfer mechanism concerning both its time and scale dependencies. In particular, we describe the so-called multifractal formalism to multitime multiscale correlation functions and what can be said about its connection with the structure of the equation of motion.

The natural set of correlation functions that one would like to control are the following:

$$C^{p,q}(r, R|t) = \left\langle \delta v_r^p(t) \cdot \delta v_R^q(0) \right\rangle, \tag{28}$$

where for the sake of simplicity, we consider velocity increments $\delta v_r(t) = v(x + r, t) - v(x, t)$ in the inertial range, and we neglect all the vectorial and tensorial dependencies. It is important to point out that the time dependence of correlations (Equation 28) is trivial whenever the velocity difference is computed in the laboratory frame of reference. In this case, the major effect is due to the sweeping of small-scale eddies by large-scale ones, which leads to correlation-times scaling as $R/\delta v_{L_0}$. The behavior of time correlations in the laboratory frame bears thus no relation to the "true" dynamical time-scale, $\tau_R \sim R/\delta v_R$, which is associated with the energy transfer. To bypass this problem, one has to get rid of sweeping: This can be accomplished by moving to a reference frame attached to a parcel of fluid in motion, a quasi-Lagrangian frame of reference (Belinicher et al. 1987). Shell models do not have sweeping, as discussed at length in the Introduction: They are a useful tool for understanding and checking nontrivial leading and subleading time dependencies in the energy cascade.

Some subclasses of multiscale multitime correlation functions (Equation 28) have recently attracted the attention of many scientists (L'vov & Procaccia 1996a, L'vov et al. 1997, Eyink 1993a, Benzi et al. 1998, Kadanoff et al. 1995, Belinicher et al. 1998). By evaluating Equation 28 with $r = R$, at changing r, and at zero-time delay $t = 0$, we have the usual structure functions of order $p+q$. Further, we may also investigate multiscale correlation functions when we have different lengths involved $r \neq R$ at zero delay, $t = 0$ as well as single-scale correlation functions by fixing $r = R$ at varying time delay t. Here we review a recent attempt (Biferale et al. 1999) to match the usual cascade modelization in terms of multiplicative random processes with the structure of the NS equations.

4.1. Background: The Multifractal Description of Time Correlations

One of the most important outcomes of experimental and theoretical analysis of turbulent flows is the spectacular ability of simple multifractal phenomenology (Frisch 1995, Parisi & Frisch 1985) to capture the leading behavior of structure functions and of multiscale correlation functions at zero-time delays (Eyink 1993a, L'vov & Procaccia 1996a, Benzi et al. 1998). More interesting were the recent findings (L'vov et al. 1997) that multifractal phenomenology may easily be extended to the time domain in such a way as to give a precise prediction on the behavior of the time properties of single scale correlations.

We remind the reader that the multifractal (Parisi & Frisch 1985) description of single-time correlation functions is based on the assumption that inertial-range statistics is fully determined by a cascade (multiplicative) process conditioned to some large-scale configuration:

$$\delta v_r = W(r, R) \cdot \delta v_R, \tag{29}$$

where the fluctuating function $W(r, R)$ can be expressed in terms of a superposition of local scaling solution $W(r, R) \sim (\frac{r}{R})^{h(x)}$ with a scaling exponent $h(x)$,

which assumes different values h in a class of interwoven fractal sets with fractal codimension $Z(h) = 3 - D(h)$. From this assumption one can write the expression for any structure functions of order m, which in our notation ($m = p + q$) becomes

$$S^m(r) \equiv C^{p,q}(r, r|0) \sim \langle W(r, L_0)^m \rangle \langle U_0^m \rangle \tag{30}$$

$$\equiv \langle U_0^m \rangle \int d\mu_{R,L_0}(h) \left(\frac{r}{L_0}\right)^{hm} \sim \left(\frac{r}{L_0}\right)^{\zeta(m)}, \tag{31}$$

where we have introduced the shorthand notation $d\mu_{R,L_0}(h) \equiv dh(\frac{r}{L_0})^{Z(h)}$ to define the probability of having a local exponent h connecting fluctuations between scales r and L_0. In Equation 31 a steepest-descent estimate was used, in the limit $r/L_0 \to 0$, in order to define the intermittent scaling exponents $\zeta(m) = \inf_h [Z(h) + mh]$. We see, therefore, that anomalous scaling is linked, by the above Legendre transform, to the existence of a whole spectrum of local exponents $h(x)$ that characterize the stochastic energy transfer along inertial scales.

Similarly, by supposing weak correlation between random function $W(r, R)$ at different scales $\langle W^p(R_1, R_2) W^q(R_2, R_3)\rangle \sim \langle W^p(R_1, R_2)\rangle \langle W^q(R_2, R_3)\rangle$, one may also write a simple "fusion-rule" prediction for simultaneous multiscale correlation functions (L'vov & Procaccia 1996b):

$$C^{p,q}(r, R|t = 0) = \langle \delta v_r^p(0) \cdot \delta v_R^q(0) \rangle \sim S^p(r)/S^p(R) S^{p+q}(R), \tag{32}$$

which is valid for all separation scales only in the fully uncorrelated approximation for the $W(r, R)$ process. As we will see, understanding the deviation to the above prediction will allow us to clarify both the phenomenological background and the analytical origins of anomalous scaling laws.

In order to extend the stochastic description to the time domain, it has been proposed (L'vov et al. 1997) that two velocity fluctuations, both at scale r but separated by a time delay t, can be characterized by the same fragmentation process $W_{r,L_0}(t) \sim W_{r,L_0}(0)$ as long as the time separation t is smaller than the instantaneous eddy-turnover time of that scale, τ_r, whereas they must be almost uncorrelated for time larger than τ_r (see Figure 7). Considering that the eddy-turnover time at scale R is itself a fluctuating quantity $\tau_r \sim r/(\delta v_r) \sim r^{1-h}$, we may write (L'vov et al. 1997)

$$C^{p,q}(r, r|t) \sim \int d\mu_{R,L_0}(h) \left(\frac{r}{L_0}\right)^{h(p+q)} F_{p,q}\left(\frac{t}{\tau_r}\right), \tag{33}$$

where the time-dependency is hidden in the function $F_{p,q}(x)$, which can be safely taken to have a simple exponential shape. From Equation 33 it is straightforward to realize that at zero-time separation we recover the usual structure-function representation. It is much more interesting to notice that Equation 33 is also in agreement with the constraints imposed by the nonlinear part of the NS equations.

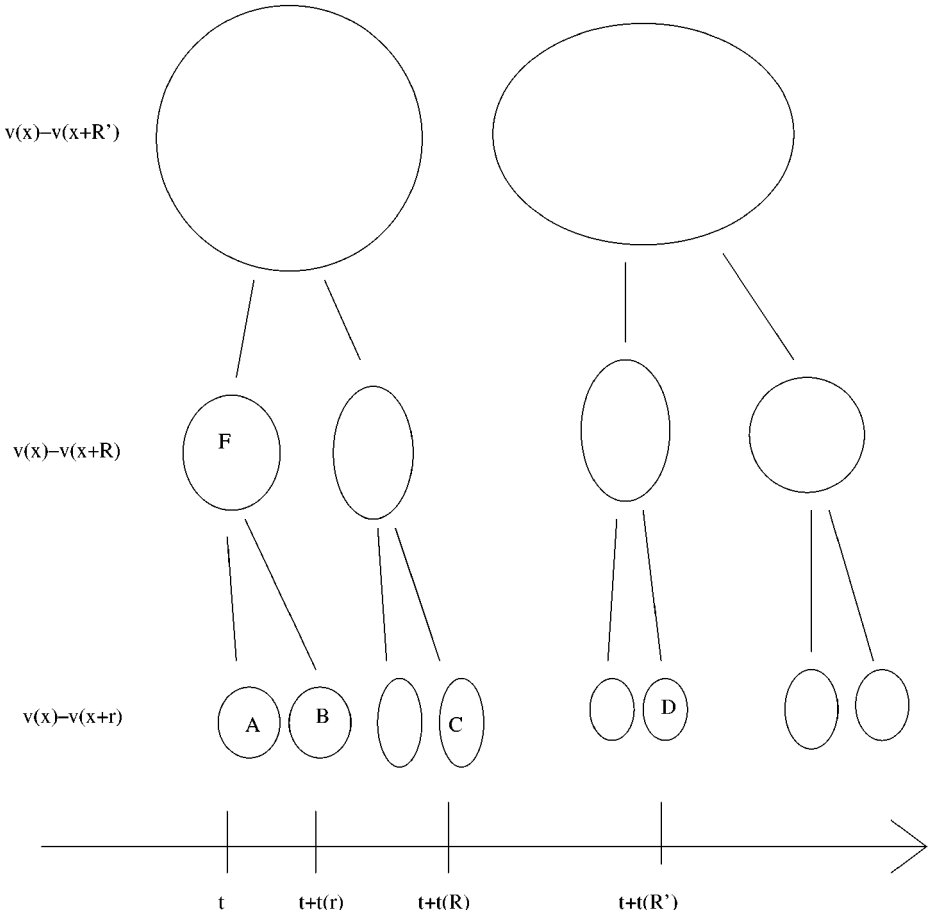

Figure 7 The time-dependent multiplicative fragmentation process. Velocity differences over a scale r are depicted by blobs. Links between blobs describe different realizations of the fragmentation process connecting fluctuations at different scales, $W(R, R')$. Time is marching on the horizontal axis. For example, blobs A and B represent the velocity increments $\delta v_r(t)$ and $\delta v_r(t + \tau_r)$, respectively. At different time lags, blobs at the same scale are correlated through older and older ancestors.

Indeed, locality of interactions implies a dimensional estimate of NS time evolution (Belinicher et al. 1998) as

$$\partial_t \delta v_r(t) \sim O\left[\frac{(\delta v_r(t))^2}{r}\right], \tag{34}$$

which is in direct agreement with what one may extract from Equation 33 once one averages all possible fluctuations:

$$\partial_t C^{p,q}(r,r|t) \sim \int d\mu_{R,L_0}(h) \left(\frac{r}{L_0}\right)^{h(p+q)} (\tau_r)^{-1} F'_{p,q}\left(\frac{t}{\tau_r}\right) \sim \frac{C^{p+1,q}(r,r|t)}{r}. \tag{35}$$

In the following we shall show how the representation Equation 33 must be improved to encompass the most general multitime multiscale correlation $C^{p,q}(r, R|t)$.

4.2. Single-Scale Time Correlations

We first show in which respect the expression of Equation 33 may not be considered a satisfactory representation of single-scale time correlation. The representation is certainly valid for short times, up to the fastest eddy-turnover time, τ_r, given by the eddy-turnover time at the scale where the velocity increments are evaluated. What must be considered, for time delay larger than τ_r, is that the ancestors (in the multiplicative sense) of the two fields at $\delta v_r(t)$ and $\delta v_r(t+t')$ start to move. For example, for times of the order of $t' \sim \tau_R$ with $R > r$, the ancestors at scale R are no longer the same in the event leading to $\delta v_r(t)$ or to $\delta v_r(t+\tau(R))$ (blobs A and C have different ancestors in Figure 7. Similarly, for times of the order of $t' \sim \tau_{R'}$, with $R' > R$, the ancestors at scale R' will start to move (blobs A and D have different ancestors up to the second generation in Figure 7).

This introduces the necessity of including corrections to Equations 33 for longer times, which depends on the whole set of hierarchical times entering into the process. Let us, for the sake of simplicity, introduce a hierarchical set of scales, $r_n = 2^{-n}$ with $n = 0, \ldots, n_d$. We also denote with $u_n = \delta v_r$ velocity fluctuation at scale $r = r_n$. Then we have a long-time description of single-scale correlation functions $C^{p,q}(r_n, r_n|t)$ given by:

$$\begin{aligned} C^{p,q}_{n,n}(t) = &\int d\mu_{n,0}(h) r_n^{(q+p)h} F_{p,q}\left(\frac{t}{\tau_n}\right) \\ &+ \sum_{m=1}^{n-1} \int d\mu_{m,0}(h)\, d\mu_{n,m}(h_1)\, d\mu_{n,m}(h_2) \\ &\times \left(\frac{r_m}{L_0}\right)^{(q+p)h} \left(\frac{r_n}{r_m}\right)^{qh_1} \left(\frac{r_n}{r_m}\right)^{ph_2} f_{p,q}\left(\frac{t}{\tau_m}\right), \end{aligned} \tag{36}$$

where the first contribution is the leading short-time term given by Equation 33, whereas the other contributions take into account subtler behavior for longer times as previously discussed. Functions $F_{p,q}(x)$ and $f_{p,q}(x)$ are smooth functions with an exponential tail describing the detailed time decaying of leading and subleading contributions. We observe that for correlation functions with a zero disconnected part, i.e., when $\lim_{t\to\infty} \langle \delta v_r^p(0) \delta v_r^q(t) \rangle \equiv 0$, the subleading terms are zero and we are left with only the form of Equation 33 (Biferale et al. 1999).

4.3. Two-Scale Time Correlations

Let us now jump to the most general multiscale multitime correlation functions,

$$C^{p,q}(r, R|t) = \left\langle \delta v_R^q(0) \cdot \delta v_r^p(t) \right\rangle, \tag{37}$$

where we denote with δv_r the velocity fluctuation at the smallest of the two scales considered, i.e., $r < R$ (see Figure 7). Now we have to consider the joint statistics of two fields: the first, the slower, at large scale $\delta v_R(0)$, and the second, the faster, at small scale and at a time delay t, $\delta v_r(t)$. As in the previous section, we use an octave-based notation $u_n = \delta v_R$ and $u_N = \delta v_r$, where it is understood that $r = 2^{-N} L_0$ and $R = 2^{-n} L_0$ (with $N > n$), denoting $C^{p,q}(r, R|t) \equiv C^{p,q}_{N,n}(t)$. Following the same reasoning as before, we may argue that there exists a leading behavior for times up to the shortest eddy-turnover time in the process, $\tau_R = \tau_n$. Notice that for a multiscale multitime correlation such as $C^{p,q}(n, N|t)$ the shortest eddy-turnover time is given by the time of the largest scale. Indeed, as can be seen in Figure 7, the velocity field at the small scale, $\delta v_r = u_N$, has the same transfer process of $\delta v_R = u_n$ up to scale R, and then from scale R to scale r an uncorrelated transfer mechanism (blobs A and B in Figure 7 have two different links to δv_R, blob F). On the other hand, for times larger than τ_R, blobs at large scales also move, and one needs to include such subleading, slower contributions:

$$\begin{aligned} C^{p,q}_{N,n}(t) = & \int d\mu_{n,0}(h)\, d\mu_{N,n}(h_1) \left(\frac{r_n}{L_0}\right)^{(q+p)h} \left(\frac{r_N}{r_n}\right)^{ph_1} F_{p,q}\left(\frac{t - T_{nN}}{\tau_n}\right) \\ & + \sum_{m=1}^{n-1} \int d\mu_{m,0}(h)\, d\mu_{n,m}(h_1)\, d\mu_{N,m}(h_2) \\ & \times \left(\frac{r_m}{L_0}\right)^{(q+p)h} \left(\frac{r_n}{r_m}\right)^{qh_1} \left(\frac{r_N}{r_m}\right)^{ph_2} f_{p,q}\left(\frac{t}{\tau_m}\right), \end{aligned} \tag{38}$$

where $T_{nN} \simeq \tau_n - \tau_N$ represents the time-delay needed for an energy burst to travel from shell n to shell N, and the functions $F_{p,q}(x)$ and $f_{p,q}(x)$ are defined in the same way as they were defined in Equation 36.

The matching of representation of Equation 38 with the equation of motion reveals many important dynamical properties (Biferale et al. 1999). Here we focus mainly on the consequences for the instantaneous multiscale correlation functions (Equation 32) because of their importance for the problem of calculating scaling exponents discussed in next section:

$$C^{p,q}(r, R|t = 0) = \left\langle \delta v_r^p(0) \cdot \delta v_R^q(0) \right\rangle = C^{p,q}_{N,n}(t = 0). \tag{39}$$

First, we notice that there is a time delay in the energy-transfer mechanism, indicated by the fact that in Equation 38, the pick of all functions f_{pq} is obtained for a time lag $O(1)$. This delay is given by the mismatch of the two eddy-turnover times of the two scales: $t_{pick} = T_{nN} = \tau_n - \tau_N$. Second, because of this time delay, we cannot expect a perfect synchronization between the multiplicative processes involving all scales. As a consequence, the simultaneous multiscale correlation

functions $C^{p,q}_{N,n}(0)$ do not show fusion-rules predictions (L'vov & Procaccia 1996b) for all scale separations, i.e., pure power-law behaviors at all scales,

$$C^{p,q}_{N,n}(0) \sim \frac{S^p_N}{S^p_n} S^{p+q}_n \sim \left(\frac{r_N}{r_n}\right)^{\zeta(p)} \left(\frac{r_n}{r_0}\right)^{\zeta(p+q)}, \tag{40}$$

where $S^p_n \equiv \langle |u_n|^p \rangle$ is the pth-order structure function. This is because for $t \to 0$, only the first term on the right-hand side survives in Equation 38, and $F_{p,q}(-\frac{T_{nN}}{\tau_n})$ can be considered a constant only within the limit of large-scale separation, $n \ll N$, whereas otherwise we will see finite-size corrections.

The delay effect in multiscale correlations is shown in Figure 8, where we compare $C^{p=1,q=1}_{N,n}(0)$ and $C^{p=1,q=1}_{N,n}(T_{nN})$ (for $N > n = 6$) rescaled with the fusion rule prediction (Equation 40). The time delay T_{nN} is the time of the maximum of $C^{1,1}_{N,n}(t)$. We see that without delay, the prediction is recovered only for $N \gg n$ with a scaling factor $F_{1,1}(-1) \simeq 0.83$, whereas by including the average delay T_{nN}, the fusion rule prediction is better verified for small-scale separation as well.

The slight derivation, for small-scale separations, still present in the upper curve of Figure 8, must be understood as the signature of some small correlation between multipliers $W(r, R)$ for small-scale separation.

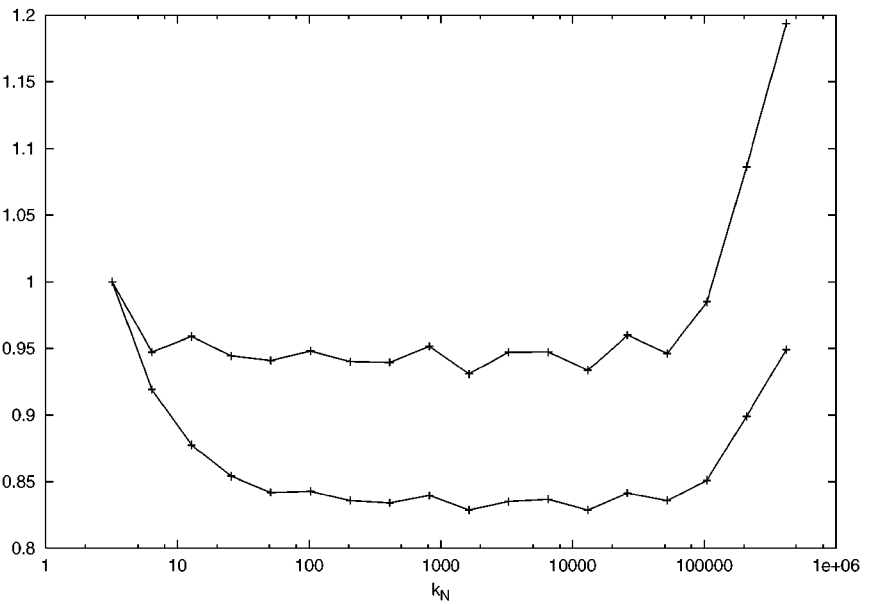

Figure 8 Lin-log plot of multiscale correlation $C^{1,1}_{n,N}(t) = \langle |u_n(0)||u_N(t)| \rangle$ rescaled with the fusion rule prediction: $C^{1,1}_{n,N}(t)/(S^1_N S^2_n / S^1_n)$ at fixed $n = 6$ and at changing $N \geq n$. The *lower line* represent the zero-delay correlation ($t = 0$); the *upper line* is for the average delay $t = \mathrm{T}_{6,N}$.

Such apparently minor points have extremely important consequences concerning the possibility of calculating from first principle, i.e., from the equation of motion, the scaling exponents. We discuss this briefly in the next subsection.

4.4. How to Calculate Anomalous Scaling Exponents

We present here a central theoretical issue: how to calculate scaling exponents in shell models. We have focused until now on a coherent phenomenological framework, based on the idea that locality in the energy cascade may well be captured by using either time-dependent stochastic (multiplicative) or dynamical (shell model) processes, or both. We have also presented numerical, experimental, and general theoretical arguments supporting the idea that anomalous scaling is a robust property of the energy cascade: It does not depend on the particular large-scale forcing and boundary conditions that we used to maintain and confine the flow. From some points of view we might be satisfied. We understand a lot about the origin of intermittency; we may understand it as the existence of zero-mode for the inertial operator, and we are able to give highly nontrivial predictions on multitime multiscale energy correlations. On the other hand, we would be even more satisfied if we could indeed calculate numbers, not only measure them. There is not space enough here to discuss the important case of Kraichnan models (Kraichnan 1994), i.e., passive scalar/vector advected by stochastic velocity fields, where indeed the goal of calculating anomalous scaling exponents is completely under control (Falkovich et al. 2001) and in many cases it has been even carried out either perturbatively or nonperturbatively in both the original hydrodynamical equations and the equivalent shell model (Kraichnan 1994, Gawedzki & Kupianen 1995, Vergassola 1996, Benzi et al. 1997).

Unfortunately, up to now, no one has been able to transfer in some solid rigorous way the vast amount of knowledge developed for the linear advection problems to the NS case. Here we discuss where the problem is for nonlinear shell models (Benzi & Biferale 2002).

Let us fix the ideas and notations by considering the exact equations derived by looking at the inertial time evolution of a typical fourth-order quantity:

$$\begin{aligned}\frac{d}{dt}\langle |u_n|^2 |u_{n+s}|^2\rangle = {} & k_n\langle W_n E_{n+s}\rangle - bk_{n-1}\langle W_{n-1}E_{n+s}\rangle \\ & + ck_{n-2}\langle W_{n-2}E_{n+s}\rangle + k_s\langle W_{n+s}E_n\rangle \\ & - bk_{n+s-1}\langle W_{n+s-1}E_n\rangle + ck_{n+s-2}\langle W_{n+s-2}E_n\rangle, \quad (41)\end{aligned}$$

where we have introduced the notation $W_n = \Im(u^*_{n+2}u_{n+1}u_n)$, $E_n = |u_n|^2$ and where we have neglected the forcing and the viscous contributions because we want to concentrate on the homogeneous inertial solutions. We now see that finding a solution in the inertial range means controlling multiscale correlation functions of the kind we have discussed in the preceeding subsection. In particular, on the basis of the multiplicative multifractal phenomenological representation setup in Section 4, we may safely give a first-order estimate of all correlation functions in

Equation 41 by using the fusion-rule predictions:

$$\langle W_{n+s} E_n \rangle = D_s \left(\frac{k_{n+s}}{k_n} \right)^{-\zeta(3)} S_n^{(5)} \quad s \geq 0 \tag{42}$$

and

$$\langle E_{n+s} W_n \rangle = F_s \left(\frac{k_{n+s}}{k_n} \right)^{-\zeta(2)} S_n^{(5)} \quad s \geq 0, \tag{43}$$

where we have introduced the fifth-order structure function $S_n^{(5)} = \langle W_n E_n \rangle$. The whole problem of finding an exact solution of Equation 41 is hidden in the two unknown functions D_s and F_s, which quantify the rate of deviation at all scales from the exact multiplicative ansatz, i.e., the rate of deviation from the fusion-rules prediction. By inserting Equations 42 and 43 in 41, one finds, after some simple algebra, three different equations, depending on whether one is on the diagonal, $s = 0$, immediately out of the diagonal, $s = 1$, or with large scale separation, $s \geq 2$:

$$\begin{aligned}
0 &= k_n^{1-\zeta(5)} \left[k_s^{-\zeta(2)} \left(D_s - bx D_{s+1} + cx^2 D_{s+2} \right) + F_s - bF_{s-1} + cF_{s-2} \right] \quad s \geq 2 \\
0 &= k_n^{1-\zeta(5)} \left[k_1^{-\zeta(2)} \left(D_1 - bx D_2 + cx^2 D_3 \right) + F_1 - bF_0 + cx D_1 \right] \quad s = 1 \\
0 &= k_n^{1-\zeta(5)} P \left[\left(D_0 - bx D_1 + cx^2 D_2 \right) + F_0 - bx D_1 + cx^2 D_2 \right] \quad s = 0,
\end{aligned} \tag{44}$$

where the unknown scaling exponents are hidden in the parameter $x = \lambda^{-1-\zeta(2)+\zeta(5)}$. What is very instructive from the preceeding equations is that one can immediately verify that the choice corresponding to an exact multiplicative uncorrelated process, i.e., $D_s = F_s = 1$ at all scales, would force the model to have as a unique solution the K41 prediction, $x = 1 \rightarrow \zeta(5) = 1 + \zeta(2)$. In other words, anomalous scaling cannot be present if fusion-rules prediction were correct for all separations of scales. Indeed, as we discussed before, fusion rules are observed for scale separations that are large enough, whereas for small-scale separation, there are important deviations due to nontrivial time properties (time delay in the energy transfer) and to some possibly weak correlations among scales.

Moreover, anomalous scaling exponents are not fixed by the asymptotic behavior of multiscale correlation functions, but by their value for close-by scales. A previous attempt was made in this direction by Benzi et al. (1993), where it was shown that one may find a multiplicative multifractal ansatz able to close with high accuracy Equation 41 (and higher-order correlation functions), at least for close-by shells, $s = 0$. The problem there was to extend the ansatz to the equations for $s > 0$, something that seems still to be out of control. There also exists a relevant case where one may accomplish the above procedure in a fully rigorous way for all orders and all scales: Benzi et al. (1997) and Anderson & Muratore-Ginanneschi (1999). This is the case of a shell model for the advection of a passive scalar by a Gaussian and delta-correlated shell-velocity field. There, if one writes down the equations like Equations in 44, one discovers that (*a*) the equations are symmetric, $D_s = F_s$, and (*b*) the recursive constraint in Equation 44 is ultraviolet stable,

i.e., one may start from large s's and integrating back, one obtains stable values for D_0 and D_1. From these values one may calculate scaling exponents by simply solving Equation 44 for $s = 0, 1$. Unfortunately, neither of the two above points is true for Equation 44. One needs some other, new, ideas.

5. A GUIDED TOUR TO FURTHER READING

Before moving on to the guided tour, let us just briefly list which of the above discussed results we consider particularly promising concerning true turbulence. Experimentally speaking, it would be of great interest to have a better control of small-scale helicity fluctuations, looking in particular for nontrivial correlation between intermittency and the helicity burst. The long discussion on decaying turbulence and its connection with the universality issue for the forcing case also looks promising for experimentalists. It would be of great interest to have a high Reynolds numbers experimental test of decaying universal properties of homogeneous turbulence looking for differences between switching off the forcing, measuring decaying properties, and starting from random (far from the attractor) initial conditions. Another key point where we lack clear experimental measurements is the whole set of multiscale, multitime correlation functions (Benzi et al. 1998, Fairhall et al. 1998), with the further problem, for the latter, avoiding sweeping effects, i.e., focusing on Lagrangian time properties (Mordant et al. 2001). As previously discussed, we have no hopes of controlling analytically the problem of anomalous scaling without a clear experimental and phenomenological control of multiscale, multitime correlation functions.

An entire interesting field we have completely ignored in this review is the application of shell models to many problems at the borderline between dynamical-systems theory and turbulence. We refer here to works done on the existence of a transition to chaos for some values of the free parameters (Biferale et al. 1995b, Kadanoff et al. 1997), to problems connected to the predictability issue (Aurell et al. 1997, Boffetta et al. 1998), to the possibility of describing the energy-cascade mechanism by exact time-reversible dynamical systems (Biferale et al. 1998c), and to some peculiar large-deviation properties of the map obtained by looking at the fixed points of the inertial terms (Biferale et al. 1994, 1997).

Theoretically speaking, shell models have also been the battleground of many interesting attempts. We cite here the renormalization-group analysis made by Eyink (1993b), the attempts to obtain a perturbative, controlled series by expanding for large N the hierarchy of correlation functions obtained by randomly coupling N identical copies of the model (Pierotti et al. 1984) or by studying the $N \to \infty$ limit of a spherical shell model (Eyink 1994, Pierotti 1997), and the recent attempt to close the hierarchy of equations by field-theoretical tools (L'vov & Procaccia 2000). Another important, and successful, field of application is connected to the study of hydrodynamical linear problems, as the passive advection of scalars and vectors by either true shell-velocity fields (Jensen et al. 1992, Brandemburg 1992, Giuliani & Carbone 1998, Arad et al. 2001, Boffetta et al. 1999) or stochastic

Gaussian and delta-correlated fields (equivalent of the Kraichnan linear advection problem) (Wirth & Biferale 1996, Benzi et al. 1997, Anserson & Muratore-Ginanneschi 1999). The latter is where the most impressive analytical understanding has been achieved. In particular, the whole ideology of zero-modes may be tested to its extreme rigorous basis for both cases when the advecting velocity is a stochastic Gaussian field (Kraichnan case) (Benzi et al. 1997, Anserson & Muratore-Ginanneschi 1999) and the more realistic case when the velocity-advecting shell fields are the outcomes of a GOY model, i.e., with highly nontrivial spatial and temporal intermittency (Arad et al. 2001). Finally, let us mention that also pulse-like solutions (instantons) have been detected and studied numerically in shell models, both in the discrete version, i.e., with intershell ratio $\lambda > 1$, (Daumont et al. 2000, Biferale et al. 1999) and in the so-called continuum limit $\lambda \to 1$, (Anderson et al. 2000).

ACKNOWLEDGMENTS

I am indebted to a huge number of colleagues for many collaborations, discussions, and arguments we have had, and still have, while working on shell models. I cannot make any explicit list: It would be too long. On the other hand, I want to honor here the memory of a friend, Giovanni Paladin, who left us a few years ago. Giovanni was a great scientist and a great human being. He was the guy who 10 years ago introduced me to shell models. I dedicate this review to his memory.

LITERATURE CITED

Andersen KH, Bohr T, Jensen MH, Nilsen JL, Olesen P. 2000. Pulses in the zero-spacing limit of the GOY model. *Phys. D* 138:44–62

Andersen KH, Muratore-Ginanneschi P. 1999. Shell model for time-correlated random advection of passive scalars. *Phys. Rev. E* 60:6663–81

Arad I, Biferale L, Celani A, Procaccia I, Vergassola M. 2001. Statistical conservation laws in turbulent transport. *Phys. Rev. Lett.* 87:164502–6

Aurell E, Boffetta G, Crisanti A, Frick P, Paladin G, Vulpiani A. 1994a. Statistical mechanics of shell models for 2-dimensional turbulence. *Phys. Rev. E* 50:4705–15

Aurell E, Boffetta G, Crisanti A, Paladin G, Vulpiani A. 1997. Predictability in the large: an extension of the concept of Lyapunov exponent. *J. Phys. A* 30:1–26

Aurell E, Frick P, Shaidurov V. 1994b. Hierarchical tree-model of 2-d turbulence. *Phys. D* 72:95–109

Belinicher VI, L'vov VS. 1987. *J. Exp. Theor. Phys.* 66:303–10

Belinicher VI, L'vov VS, Pomyalov A, Procaccia I. 1998. Computing the scaling exponents in fluid turbulence from first principles: demonstration of multiscaling. *J. Stat. Phys.* 93:797–832

Benzi R, Biferale L. 2002. Intermittency in turbulence. *Proc. CISM School, Theory Turbul.* In press

Benzi R, Biferale L, Parisi G. 1993. On intermittency in a cascade model for turbulence. *Phys. D* 65:163–71

Benzi R, Biferale L, Kerr R, Trovatore E. 1996a. Helical-shell models for three-dimensional turbulence. *Phys. Rev. E* 53:3541–50

Benzi R, Biferale L, Succi S, Toschi F. 1999. Intermittency and eddy-viscosities in dynamical models of turbulence. *Phys. Fluids* 11:1221–28

Benzi R, Biferale L, Toschi F. 1998. Multiscale correlation functions in turbulence. *Phys. Rev. Lett.* 80:3244–48

Benzi R, Biferale L, Tripiccione R, Trovatore E. 1996b. $(1+1)$-dimensional turbulence. *Phys. Fluids* 9:2335–63

Benzi R, Biferale L, Wirth A. 1997. Analytic calculation of anomalous scaling in random shell models for a passive scalar. *Phys. Rev. Lett.* 78:4926–29

Benzi R, Ciliberto S, Baudet C, Ruiz Chavarria G. 1995. On the scaling of three-dimensional homogeneous and isotropic turbulence. *Phys. D* 80:385–98

Benzi R, Paladin G, Parisi G, Vulpiani A. 1984. On the multifractal nature of fully developed turbulence and chaotic systems. *J. Phys. A* 17:3521–31

Biferale L, Blank M, Frisch U. 1994. Chaotic cascades with Kolmogorov 1941 scaling. *J. Stat. Phys.* 75:781–95

Biferale L, Boffetta G, Celani A, Lanotte A, Toschi F, Vergassola M. 2002. Isotropic and anisotropic decaying turbulence. *Phys. Rev. Lett.* Submitted

Biferale L, Boffetta G, Celani A, Toschi F. 1999. Multi-time multi-scale correlation function in turbulence and in turbulent models. *Phys. D* 127:187–97

Biferale L, Cencini M, Pierotti D, Vulpiani A. 1997. Intermittency in stochastically perturbed turbulent models. *J. Stat. Phys.* 88:1117–38

Biferale L, Daumont I, Dombre T, Lanotte A. 1999. Coherent structures in random shell models for passive scalar advection. *Phys. Rev. E* 60:R6299–302

Biferale L, Kerr R. 1995. Role of inviscid invariants in shell models of turbulence. *Phys. Rev. E* 52:6113–22

Biferale L, Lambert A, Lima R, Paladin G. 1995b. Transition to chaos in a shell model of turbulence. *Phys. D* 80:105–19

Biferale L, Pierotti D, Toschi F. 1998a. Helicity advection in turbulent models. *J. Phys.* 8:131–37

Biferale L, Pierotti D, Toschi F. 1998b. Helicity transfer in turbulent models. *Phys. Rev. E* 57:R2515–18

Biferale L, Pierotti D, Vulpiani A. 1998c. Time-reversible dynamical systems in turbulence. *J. Phys. A* 31:21–32

Boffetta G, Carbone V, Giuliani P, Veltri P, Vulpiani A. 1999. Power laws in solar flares: self-organized criticality or turbulence? *Phys. Rev. Lett.* 83:4662–65

Boffetta G, Giuliani P, Paladin G, Vulpiani A. 1998. An extension of the Lyapunov analysis for the predictability problem. *J. Atmos. Sci.* 55:3409–16

Bohr T, Jensen MH, Paladin G, Vulpiani A. 1998. *Dynamical Systems Approach to Turbulence*. Cambridge, UK: Cambridge Univ. Press

Borue V, Orszag SA. 1995. Force three-dimensional homogeneous turbulence with hyperviscosity. *Europhys. Lett.* 29:687–90

Borue V, Orszag SA. 1997. Spectra in helical three-dimensional homogeneous isotropic turbulence. *Phys. Rev. E* 55:7005–9

Brandemburg A. 1992. Energy spectra in a model for convective turbulence *Phys. Rev. Lett.* 69:605–8

Cao N, Chen S, She SZ. 1996. Scalings and the relative scalings in Navier-Stokes turbulence. *Phys. Rev. Lett.* 76:3711–14

Chkhetiani O. 1996. On the triple correlations in helical turbulence *JETP Lett*. 63:808–12

Daumont I, Dombre T, Gilson JL. 2000. Instanton calculus in shell models of turbulence. *Phys. Rev. E* 62:3592–610

Desnyansky VN, Novikov EA. 1974. The evolution of turbulence spectra to the similarity regime. *Izv. Akad. Nauk. SSSR Fiz. Atmos. Okeana* 10:127–36

Ditlevsen PD. 1997. Cascades of energy and helicity in the GOY shell model of turbulence. *Phys. Fluids* 9:1482–84

Ditlevsen PD, Mogensen IA. 1996. Cascades and statistical equilibrium in shell models of turbulence. *Phys. Rev. E* 53:4785–93

Eggers J, Grossman S. 1991. Anomalous turbulent velocity scaling from the Navier-Stokes equation. *Phys. Lett. A* 156:444–49

Eyink G. 1993a. Lagrangian field-theory, multifractals and universal scaling in turbulence. *Phys. Lett. A* 172:355–60

Eyink G. 1993b. Renormalization group and operator product expansion in turbulence-shell models. *Phys. Rev. E* 48:1823–38

Eyink G. 1994. Large-N limit of the spherical model of turbulence. *Phys. Rev. E* 49:3990–4002

Fairhall AL, L'vov VS, Procaccia I. 1998. Dissipative scaling functions in Navier-Stokes turbulence: experimental tests. *Europhys. Lett.* 43:277–83

Falkovich G, Gawedzki K, Vergassola M. 2001. Particles and fields in fluid turbulence. *Rev. Mod. Phys.* 73:913–75

Frick P, Dubrulle B, Babiano A. 1995. Scaling properties of a class of shell models. *Phys. Rev. E* 51:5582–93

Frisch U. 1995. *Turbulence: The Legacy of A.N. Kolmogoro*. Cambridge, UK: Cambridge Univ. Press

Gawedzki K, Kupiainen A. 1995. Anomalous scaling of the passive scalar. *Phys. Rev. Lett* 75:3834–37

Giuliani P, Carbone V. 1998. A note on shell models for MHD turbulence. *Europhys. Lett.* 43:527–32

Gledzer EB. 1973. System of hydrodynamic type admitting two quadratic integrals of motion. *Sov. Phys. Dokl.* 18:216–17

Grossmann S, Lohse D. 1994. Scale resolved untermittency in turbulence. *Phys. Fluids A* 6:611–17

Jensen MH, Paladin G, Vulpiani A. 1991. Intermittency in a cascade model for 3-dimensional turbulence. *Phys. Rev. A* 43:798–805

Jensen MH, Paladin G, Vulpiani A. 1992. Shell model for turbulent advection of passive-scalar fields. *Phys. Rev. A* 45:7214–21

Kadanoff L, Lohse D, Schorghofer N. 1997. Scaling and linear response in the GOY turbulence model. *Phys. D* 100:165–86

Kadanoff L, Lohse D, Wang J, Benzi R. 1995. Scaling and dissipation in the GOY shell model. *Phys. Fluids* 7:617–29

Kolmogorov AN. 1962. A refinement of previous hypothesis concerning the local structyure of turbulence in a viscous incompressible fluid at high Reynolds number. *J. Fluid Mech.* 13:82–85

Kraichnan RH. 1994. Anomalous scaling of a randomly advected passive scalar. *Phys. Rev. Lett.* 72:1016–19

Landau LD, Lifshitz EM. 1987. *Fluid Mechanics*. Oxford: Pergamon. 2nd ed.

Lorenz EN. 1972. Deterministic nonperiodic flow. *J. Atmos. Sci.* 20:130–41

L'vov V, Podivilov E, Pomyalov A, Procaccia I, Vandembroucq D. 1998a. Improved shell model of turbulence. *Phys. Rev. E* 58:1811–22

L'vov VS, Podivilov E, Procaccia I. 1997. Temporal multiscaling in hydrodynamic turbulence. *Phys. Rev. E* 55:7030–35

L'vov VS, Procaccia I. 1996a. Fusion rules in turbulent systems with flux equilibrium. *Phys. Rev. Lett*. 76:2898–901

L'vov VS, Procaccia I. 1996b. Towards a nonperturbative theory of hydrodynamic turbulence: Fusion rules, exact bridge relations, and anomalous viscous scaling functions. *Phys. Rev. E* 54:6268–84

L'vov SV, Procaccia I. 2000. Analytic calculation of the anomalous exponents in turbulence: using the fusion rules to flush out a small parameter. *Phys. Rev. E* 62:8037–57

L'vov VS, Procaccia I, Vandembroucq D. 1998b. Universal scaling exponents in shell models of turbulence: viscous effects are finite-sized corrections to scaling. *Phys. Rev. Lett.* 81:802–5

Mandelbrot B. 1977. Intermittent turbulence in self-similar cascades: divergence of high moments and dimension of the carrier. *J. Fluid Mech.* 62:331–58

Meneveau C, Sreenivasan KR. 1987. The multifractal spectrum of the dissipation field in

turbulent flows. *Nucl. Phys. B Proc. Suppl.* 2:49–76

Moffat HK. 1969. The degree of knotedness of tangled vortex lines. *J. Fluid Mech.* 35:117–29

Moffat HK, Tsinober A. 1992. Helicity in laminar and turbulent flows. *Annu. Rev. Fuid Mech.* 24:281–312

Mordant N, Metz P, Michel O, Pinton JF. 2001. Measurement of Lagrangian velocity in fully developed turbulence. *Phys. Rev. Lett.* 87:214501–4

Muzy JF, Bacry E, Arneodo A. 1993. Multifractal formalism for fractal signals: the structure functions approach versus the waelet-transform modulus-maximum method. *Phys. Rev. E* 47:875–84

Nakano T. 1988. Direct interaction approximation of turbulence in the wave packet representation. *Phys. Fluids* 31:1420–28

Noullez A, Wallace G, Lempert W, Miles RB, Frisch U. 1997. Transverse velocity increments in turbulent flow using the RELIEF technique. *J. Fluid Mech.* 339:287–307

Ohkitani K, Yamada M. 1989. Temporal intermittency in the energy cascade process and local Lyapunov analysis in fully developed model of turbulence. *Prog. Theor. Phys.* 89:329–41

O'Neil J, Meneveau C. 1993. Spatial correlations in turbulence: predictions from the multifractal formalism and comparison with experiments. *Phys. Fluids A* 5:158–72

Parisi G, Frisch U. 1985. On the singularity structure of fully deeloped turbulence. In *Turbulence and Predictability in Geophysical Fluid Dynamics*, ed. M Ghil, R Benzi, G Parisi, pp. 84–87. Varenna: Int. School Phys.

Pierotti D. 1997. Intermittency in the large N-limit of a spherical shell model for turbulence. *Europhys. Lett.* 37:323–28

Pierotti D, L'vov VS, Pomyalov A, Procaccia I. 2000. Anomalous scaling in a model of hydrodynamic turbulence with a small parameter. *Europhys. Lett.* 50:473–79

Pisarenko D, Biferale L, Courvoisier D, Frisch U, Vergassola M. 1993. Further results on multifractality in shell models. *Phys. Fluids A* 5:2533–38

Pope SB. 2000. *Turbulent Flows*. Cambridge, UK: Cambridge Univ. Press

Renner C, Peinke J, Friedrich R. 2001. Experimental indications for Markov properties of small-scale turbulence. *J. Fluid Mech.* 433:383–409

Siggia ED. 1978. Model of intermittency in three-dimensional turbulence. *Phys. Rev. A* 17:1166–76

Stolovitzky G, Sreenivasan KR. 1994. Kolmogorov's refined similarity hypothesis for turbulence and general stochastic processes. *Rev. Mod. Phys.* 66:229–40

van de Water W, Herweijer J. 1996. Anomalous scaling and anisotropy in turbulence *Phys. Scr. T* 67:136–40

Vergassola M. 1996. Anomalous scaling for passively advected magnetic fields. *Phys. Rev. E* 53:R3021–24

Waleffe F. 1992. The nature of triad interactions in homogeneous turbulence. *Phys. Fluids* 4:350–63

Waleffe F. 1993. Inertial transfers in the helical decomposition *Phys. Fluids* 5:677–85

Wirth A, Biferale L. 1996. Anomalous scaling in random shell models for passive scalars. *Phys. Rev. E* 54:4982–89

Annual Review of Fluid Mechanics
Volume 35, 2003

CONTENTS